

Graph in Graph Neural Network

Jiongshu Wang¹, Jing Yang³, Jiankang Deng², Hatice Gunes³, Siyang Song^{1,3*}

¹School of Computing and Mathematical Sciences, University of Leicester, Leicester, LE1 7RH, East Midlands, United Kingdom.

²Department of Computing, Imperial College London, London, SW7 2AZ, London, United Kingdom.

³Department of Computer Science and Technology, University of Cambridge, Cambridge, CB3 0FD, Cambridgeshire, United Kingdom.

*Corresponding author(s). E-mail(s): ss2796@cam.ac.uk;

Contributing authors: jiongshuwang@gmail.com; y.jing2016@gmail.com;
jiankangdeng@gmail.com; Hatice.Gunes@cl.cam.ac.uk;

Abstract

Existing Graph Neural Networks (GNNs) are limited to process graphs each of whose vertices is represented by a vector or a single value, limited their representing capability to describe complex objects. In this paper, we propose **the first GNN (called Graph in Graph Neural (GIG) Network)** which can process graph-style data (called GIG sample) whose vertices are further represented by graphs. Given a set of graphs or a data sample whose components can be represented by a set of graphs (called multi-graph data sample), our GIG network starts with a GIG sample generation (GSG) module which encodes the input as a **GIG sample**, where each GIG vertex includes a graph. Then, a set of GIG hidden layers are stacked, with each consisting of: (1) a **GIG vertex-level updating (GVU)** module that individually updates the graph in every GIG vertex based on its internal information; and (2) a **global-level GIG sample updating (GGU)** module that updates graphs in all GIG vertices based on their relationships, making the updated GIG vertices become global context-aware. This way, both internal cues within the graph contained in each GIG vertex and the relationships among GIG vertices could be utilized for down-stream tasks. Experimental results demonstrate that our GIG network generalizes well for not only various generic graph analysis tasks but also real-world multi-graph data analysis (e.g., human skeleton video-based action recognition), which achieved the new state-of-the-art results on 13 out of 14 evaluated datasets. Our code is publicly available at <https://github.com/wangjs96/Graph-in-Graph-Neural-Network>.

Keywords: Graph Neural Network, Vertex representation, Message passing, Multi-graph data

1 Introduction

Graph Neural Networks (GNNs) [1] are deep neural networks specifically designed to process graph-structured data. Recent advances in GNNs (e.g., Graphormer [2], EGNN [3], SIGN [4] and GatedGCN [5]) can effectively extract task-specific features from non-Euclidean graphs (e.g., Graph data, Tree structures, Manifolds and Mesh networks), where each graph vertex describes the mathematical abstraction of an object [6]. Consequently, GNNs have been successfully developed for a diverse range of real-world applications such as social network analysis [7, 8], drug discovery [9], recommendation systems

[10, 11], object recognition and segmentation [12–15], and human behaviour understanding [16–22].

To extract task-specific patterns from graph vertices and their connections (i.e., edges) for analysis, most early GNNs [23–26] were built upon anisotropic operations, which updates vertices based on their first-order vertex neighbours, while others [26–31] extended Convolution Neural Networks (CNNs) to the graph domain, allowing each vertex to exchange messages with its higher-order neighbours. Recently, more advanced GNNs are proposed to process graphs that have not only different typologies (heterogeneous graphs), e.g., Heterogeneous Graph Neural Network [32], Heterogeneous Graph Attention Network [33], etc., but also multi-dimensional edge features (e.g.,

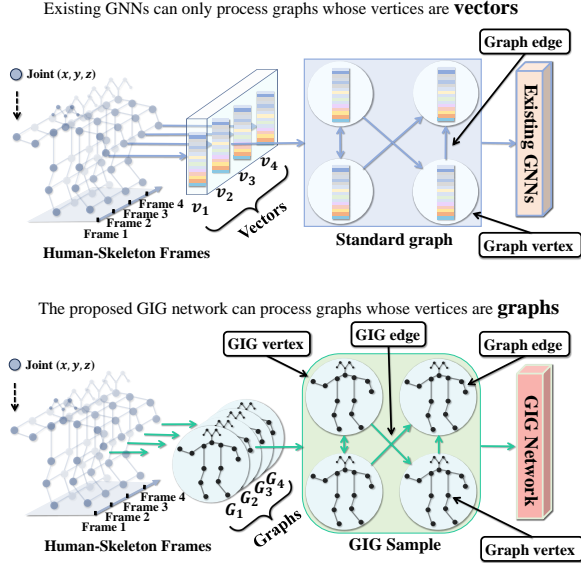


Fig. 1: Comparison between existing GNNs and our GIG network based on the example of human skeleton video-based action recognition task. While **existing GNNs** can only process graphs whose vertices carrying *vectors or single values*, they require to reduce each graph-style human skeleton frame as a vector. Our approach can directly include every graph-style frame in a GIG vertex in the proposed GIG sample, which is then processed by our GIG network that can process GIG samples whose vertices carrying *more comprehensive graphs*.

EGNNs [34], ME-GCN [35], and MDE-GNN [36], etc.), aiming for more comprehensive and effective vertex and edge feature extraction/updating. Dwivedi et al. [37] further integrated the advanced heterogeneous graph and multi-dimensional edge feature processing mechanisms into several widely-used GNNs (e.g., Graph Attention Network (GAT) [38], Gated Graph ConvNets (GatedGCN) [39], etc.).

While there have been significant advancements in vertex and edge updating mechanisms for recent GNNs, to the best of our knowledge, no previous work has attempted to enhance another crucial aspect of GNNs, i.e., their vertex representing capability, which enables these GNNs to process more structured vertex representations (i.e., graphs). More specifically, since existing GNNs can only handle vertices represented by single values or vectors of a fixed dimension, previously proposed GNN-based real-world data analysis approaches largely depend on a data-specific pre-processing step that transform the target real-world data sample (e.g., video frame [16]) of the data sample is usually encoded as a graph vertex represented by either a vector or a single value. This restricts the capability of GNNs to handle more complex scenarios, such as those where multiple complex objects are presented (e.g., a video consisting of multiple human face or skeleton frames),

i.e., when representing each human face or skeleton, a graph may be a more powerful representation than a vector/value [17, 40, 41] (**Motivation 1**). Additionally, recent studies found that the relationships among graph samples in the same dataset can provide crucial cues to further enhance their analysis performance (i.e., enhancing performances for generic graph analysis tasks) [42, 43], where contrastive learning strategies have been frequently extended to model such relationships [44]. Such strategies usually utilize loss functions to maximise the similarity among graphs/vertices belonging to the same category while minimising the similarity among graphs belonging to the different categories, which are limited to model a specific relationship among graphs based on the manually-defined loss function. As a result, a more effective, comprehensive and task-specific strategy for modelling the relationship among graphs may further improve GNNs' performances in generic graph analysis tasks (**Motivation 2**).

In this paper, we propose a novel **Graph in Graph (GIG) Neural Network** which can process a more comprehensive graph-style data structure (called **GIG sample**) whose vertices can carry more powerful representations (i.e., graphs). The proposed GIG network is flexible to incorporate advanced vertex and edge updating functions from various existing GNNs, making it capable of handling GIG samples carrying multiple heterogeneous graphs and graphs containing multi-dimensional edge features. The comparison between the proposed GIG network and existing GNNs are visualised in Fig. 1. Our GIG network starts with a **GIG sample generation (GSG) layer** which encodes the input data sample (a batch of graphs or a non-graph data sample whose components can be effectively represented by multiple graphs (called multi-graph data sample in this paper)) as a GIG sample consisting of multiple GIG vertices, where each vertex contains a graph. Then, a set of **GIG hidden layers** are stacked, where each is composed of two modules: a GIG vertex updating (GVU) module that independently updates the graph in each GIG vertex based on its internal information, and a global-level GIG sample updating (GGU) module that updates the graph in each GIG vertex based on its relationships with graphs in other GIG vertices. Finally, a **GIG output layer** is attached to produce the updated local and global context-aware GIG latent representation. The full pipeline of our GIG network is also illustrated in Fig. 2. The main contributions and novelties of this paper are summarised as follows:

- The proposed GIG Network is a large improvement over existing GNNs, as it can process graph-style data (i.e., GIG samples) whose vertices can carry more structured representations (i.e., graphs). This diverges from existing GNNs [26, 32, 33, 37, 39]

that can only handle graphs with vertices containing vectors or single values (**Novelty 1**).

- We propose a novel and efficient two-stage updating strategy to define the GIG hidden layer, where GVV and GGU modules can repeatedly and explicitly learn both internal cues within the graph contained in each GIG vertex as well as the relationship cues between graphs in different GIG vertices in an end-to-end manner. This enables our GIG network to process complex scenarios where each data sample can be effectively described by multiple graphs (**Novelty 2**).
- Our GIG network is suitable for analyzing real-world multi-graph data (i.e., a data sample that can be effectively represented by multiple graphs), as well as a batch of graph samples for generic graph analysis tasks, where each input graph is contained in a GIG vertex. This differs from existing sub-graph GNNs [45–50] which divide each input graph into multiple sub-graphs. The results show that our GIG network achieved state-of-the-art performances on 13 out of 14 datasets, highlighting its potential for a broad range of graph analysis tasks.

2 Related Work

2.1 Graph Neural Networks

Graph Neural Networks (GNNs) are effective models to process graph-structured data, which models the intricate patterns and relationships inherent within graphs. Existing GNNs can be categorized as Message Passing GNNs (MPNNs) and Weisfeiler Lehman GNNs [37]. Specifically, MPNNs usually aggregate feature information from each vertex’s nearest neighbours to update its state, potentially followed by a nonlinear transformation. For example, the Graph Convolution Network (GCN) [51] is built on a straightforward message-passing mechanism, which aggregates information from each vertex’s neighbouring vertices to update it. GraphSAGE [52] extends such neighbour aggregation mechanism by learning a function for inductive feature aggregation from each vertex’s local neighbouring vertices. Graph Attention Network (GAT) [53] introduces an attention mechanism to weigh neighbours’ contributions dynamically. Simple Graph Convolution (SGC) [54] simplifies the attention calculation by condensing consecutive convolutional layers into a single linear transformation, aiming to reduce computational demands. Jumping Knowledge Networks (JKN) [55] offer flexibility in aggregation by allowing features from various sizes of neighbour to be combined, to address the commonly faced over-smoothing issue in MPNNs. However, these MPNNs usually suffer from scalability challenges and might struggle with capturing global graph properties as they are focusing on local information aggregation.

Weisfeiler-Lehman GNNs (WLGNNs), on the other hand, push the boundaries of graph representation learning by capturing higher-order structural information. A typical example is the Graph Isomorphism Network (GIN) [56] which maximizes the representational limit to match the Weisfeiler-Lehman isomorphism test, and thus enables the distinction of complex graph structures. Besides, K-GNN [57] expands maximization mechanism by generalizing the aggregation mechanism to higher-order vertex tuples, which can encapsulate more detailed structural information. DGCNN [58] is proposed for point clouds analysis, which adapts the Weisfeiler-Lehman (WL) principle to sort the vertex features in a way that corresponds to the order implied by the WL test. PAN [59] enhances the learning capacity of GNNs by augmenting graph structures with paths that encapsulate higher-order connectivity patterns, which is similar to the WL kernel’s attempt. This allows it to capture more complex graph structures beyond the nearest neighbours as the way employed in the GCN. Despite the advanced capabilities in capturing detailed and nuanced graph features, WLGNNs generally face the challenges including the increased computational demands as well as the higher probability to trigger overfitting during their training. Such drawbacks may make them harder to be implemented and optimized compared to their MPNNs counterparts.

2.2 Graph vertex representation learning

To utilise GNNs for real-world data analysis, a large number of graph representation learning strategies have been proposed to represent various types of data as graphs, where the key component/objects in the target data are usually represented as vertices in the graph. In the realm of graph-based image analysis, each image region or region containing an object is typically treated as a vertex feature vector. For example, Li et al. [60] and Han et al. [61] propose scene graph generation approaches, where the image patch of each object in the scene image is encoded as a vertex vector in the corresponding scene graph, which are then processed by a GNN to model each scene’s layout and its object interactions. Wang et al. [62] introduce a graph-based video action recognition approach which represents each video as a graph. Specifically, each video frame (i.e., an image) is represented as a vertex feature vector in the graph. These vertices are then connected based on the temporal proximity of the corresponding frames and the similarity of their contents, to model their temporal relationships. Similar strategies have been proposed by Yan et al. [16] and Chen et al. [63], which also represent each video frame as a vertex vector in the graph. While spatial cues and relationships between different objects/components contained in

each image patch or each video frame may be crucial for the downstream analysis, representing these cues within a vector may lead to significant information loss or distortion, and thus limit GNNs’ analysis performances.

Graphs also have been used to represent audio data as valuable relationship exists among audio segments. In the work by Purwins et al. [64], a graph-based representation for music recommendation systems was proposed. Features of audio segments are extracted using signal processing techniques and then encoded into vectors to generate vertices. Similarly, An et al. [65], Zhang et al. [66] and Singh [67] also generated vertices through directly encoding each audio segment as a vertex feature vector. While each audio segment typically possesses the abundant types of features extracted from different perspectives [68, 69], e.g., the time domain, the frequency domain and the Mel-Spectrogram etc, compressing all types of features within a vector could cause GNNs failing to well explore relationships among features extracted from different perspectives during the propagation, and thus limit their learning capability. Besides, graphs can also represent documents. For instance, Huang et al. [70] introduced a graph-based text summarization method, where each sentence is encoded as a vertex feature vector. However, structural relationships (e.g., semantic characteristics, emotional status, or logical coherence) among words in each sentence could not be well represented within a vector, i.e., important contextual cues would be losing before the formal learning stage starts.

3 Preliminaries

Given a graph sample $\mathcal{G}(V, E)$, where V is a set of vertices with $v_n \in V$ and E is a set of edges connecting adjacent vertices, existing message-passing GNN (MPNN) layers usually output an updated graph $\hat{\mathcal{G}}(\hat{V}, \hat{E})$ as:

$$\hat{\mathcal{G}}(\hat{V}, \hat{E}) = f(\mathcal{G}(V, E), A), \quad (1)$$

where A is an adjacent matrix describing the topology of $\mathcal{G}(V, E)$. Each edge connecting vertex v_n to v_m is represented by $e_{n,m} = (v_n, v_m) \in E$. The generic function for updating each edge feature $e_{n,m}$ can be formulated as:

$$\hat{e}_{n,m} = \begin{cases} f_e(e_{n,m}, v_n, v_m) & \text{Updating edge} \\ e_{n,m} & \text{Otherwise} \end{cases} \quad (2)$$

where f_e is a differentiable edge feature updating function fed with the initial edge feature $e_{n,m}$ and corresponding vertex features v_n and v_m . By updating all edges, the updated edge feature set \hat{E} is obtained. Here, some GNNs (e.g., vanilla GCN [51],

AdaGPR [71], GATv2 [72]) do not update edge feature, and thus the input and output graphs share same edge features. Then, each vertex feature v_n is updated as:

$$\begin{aligned} \hat{v}_n &= f_v(v_n, \mathbf{m}_{\mathcal{N}(v_n)}), \\ \mathbf{m}_{\mathcal{N}(v_n)} &= \text{Agg}(g_v(v_m, \hat{e}_{n,m}) | v_m \in \mathcal{N}(v_n)) \end{aligned} \quad (3)$$

where f_v is a differentiable vertex updating function that takes v_n and its adjacent vertices $\mathcal{N}(v_n)$ as the input, while the operation Agg involves aggregating the information passed from adjacent vertices in a graph. Here, each adjacent vertex v_m affects the target vertex v_n via the edge that connects them, represented as $e_{m,n}$, and the the impact is also determined by the function g_v .

4 Graph in Graph Neural Network

This section presents our novel GIG network. As demonstrated in Fig. 2 and Algorithm 1, it starts with a **GIG Sample Generation (GSG)** layer (Sec. 4.1), which transforms an arbitrary input data \mathcal{D} to a GIG sample $\mathcal{G}(\mathcal{S}, P_l, P_g, E_P, E_G)$. In an obtained GIG sample, each key component/object of the input data is summarised in a graph contained in a GIG vertex $\mathcal{S}^i(V_S^i, E_S^i) \in \mathcal{S}$. Besides, this module also defines a local proxy vertex $P_l^i \in P_l$ (represented as a vector or a single value) to summarise the graph contained in each GIG vertex, as well as a global proxy vertex $P_g^i \in P_g$ aiming at collecting global and contextual information from graphs contained in other GIG vertices. To facilitate message exchanging among GIG vertices, the GSG layer initialises a set of undirected GIG edges $e^{i,j} \in E_G$ to connect each pair of GIG vertices via their local and global proxy vertices. Then, a set of **GIG hidden layers** are stacked to process the GIG sample output from the GSG layer, with each composed of a GIG vertex level updating (GVU) module (Sec. 4.2.1) and a global-level GIG sample updating (GGU) module (Sec. 4.2.2). The GVU module individually updates the graph contained in each GIG vertex by leveraging the internal (local) information within the graph, while the GGU module (Sec. 4.2.2) updates each GIG vertex based on its relationship with other GIG vertices, thereby updating GIG edges connecting GIG vertices. Finally, a **GIG output layer** is attached at the top of the GIG network to produce the final prediction.

4.1 GIG sample generation (GSG) layer

GIG sample definition. We first introduce a novel graph-style structure called Graph in Graph (GIG) sample (denoted as \mathcal{G}), which is made up of a

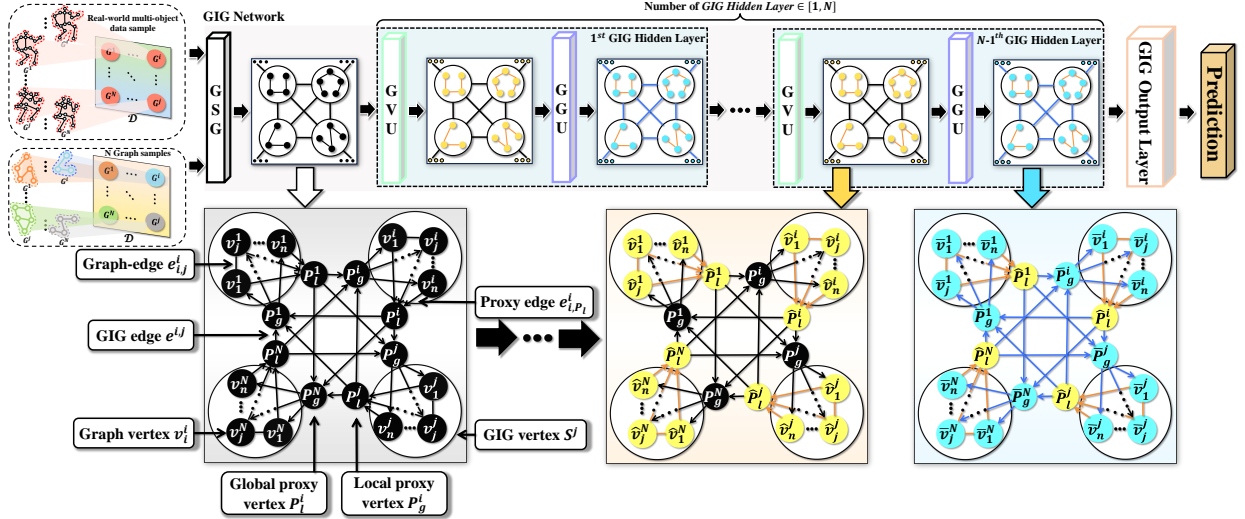


Fig. 2: Illustration of the propagation of the **GIG** network. Given a real-world multi-graph sample or a set of graph samples as the input, the GSG layer first transforms the input as a **GIG** sample, where each graph/graph sample is represented by a **GIG** vertex and each **GIG** vertex is represented by a proxy vertex. Then, a set of **GIG** layers are stacked, where each consists of (i) a **GVU** module which individually updates each **GIG** vertex (i.e., its graph edges, graph vertices, directed proxy edges starting from graph vertices, and local proxy vertex) based on its internal cues; and (ii) a **GGU** module which further updates each **GIG** vertex based on its relationship with other **GIG** vertices (i.e., updating global-edges, global proxy vertices, directed proxy edges starting from global proxy vertices, and graph vertices).

set of **GIG** vertices \mathcal{S} and **GIG** edges E_G . Specifically, each **GIG** vertex $S^i \in \mathcal{G}$ contains a graph $S^i(V_S^i, E_S^i)$ that is made up of N_i vertex vectors $V_S^i = \{v_1^i, v_2^i, \dots, v_{N_i}^i\}$ (called graph vertices in this paper), and a set of edges (called graph edges in this paper), where each graph edge $e_{n,m}^i \in E_S^i$ connects a pair of graph vertices v_n^i and v_m^i in S^i (illustrated in Fig. 2). To facilitate efficient communication between graphs contained in different **GIG** vertices, the **GIG** sample also defines a local proxy vertex $P_l^i \in P_l$ and a global proxy vertex $P_g^i \in P_g$ for each **GIG** vertex S^i , where P_l^i integrates local features from the graph contained in S^i , while the global proxy vertex P_g^i receives contextual cues from other **GIG** vertices, aiming to further pass them to update graph vertices of the S^i . As a result, each local proxy vertex P_l^i / global proxy vertex P_g^i is linked to a set of graph vertices contained in its **GIG** vertex S^i (e.g., directed edge e_{n,P_l}^i from the graph vertex v_n^i to local proxy vertex P_l^i / directed edge $e_{P_g,n}^i$ from global proxy vertex P_g^i to the graph vertex v_n^i). Meanwhile, each pair of connected **GIG** vertices S^i and S^j exchange messages via a pair of directed global-edges $e_{i,j} \in E_G$ and $e_{j,i} \in E_G$, where $e_{i,j}$ starts from the local proxy vertex P_l^i of S^i to the global proxy vertex P_g^j of S^j passes the cues of S^i to the **GIG** vertex S^j . Thus, a **GIG** sample can be represented as $\mathcal{G}(S_G(V_S, E_S), P_l, P_g, E_P, E_G)$. The definitions of employed notations are listed in Table 1.

GSG layer. The GSG layer transforms an arbitrary input data sample \mathcal{D} (i.e., real-world multi-graph data or a batch of graph samples) to a **GIG** sample accordingly, where each **GIG** vertex contains either a graph representation representing an object/-component of the input multi-graph data or a graph sample of the input graph batch. For example, for human skeleton video-based action recognition tasks, each human skeleton frame will be summarised as a graph and contained in a **GIG** vertex. Consequently, the **GIG** sample is constructed on the basis of multiple frames, with each **GIG** vertex representing a skeleton frame. For generic graph analysis tasks, a batch of graph samples will be combined as a **GIG** sample, with each **GIG** vertex containing a graph sample. After defining all **GIG** vertices, the GSG layer initialises each local proxy vertex P_l^i by averaging all graph vertices in its corresponding **GIG** vertex S^i , and each global proxy vertex P_g^i as a zero vector. Then, the GSG defines a set of directed proxy edges to connect a set of graph vertices with its corresponding local proxy vertex P_l^i and global proxy vertex P_g^i , and initialises them as zero vectors. For each **GIG** vertex, its proxy edges are connected: (i) from a set of its graph vertices that are least similar to its local proxy vertex; and (ii) from its global proxy vertex to a set of its graph vertices that are most similar to the local proxy vertex, where cosine similarity is empirically used in this paper (the influence of different similarity measurements are evaluated in Supplementary Material). The experimental analysis for various connection strategies are reported

Algorithm 1 Pseudocode of the GIG network propagation

Input: A original multi-graph data sample or a set of graph samples $\mathcal{D} = \{S^1, \dots, S^I\}$.

Output: An updated GIG sample consisting of I GIG vertices: $\bar{\mathcal{G}}^L(\bar{S}_G(\bar{V}_S, \bar{E}_S), \bar{P}_g, \bar{E}_P, \bar{E}_G)$

Model: GIG network equipped with a GSG layer, L hidden GIG layers, and an output GIG layer.

The propagation process of the GIG network:

GSG layer: Producing a GIG sample from the input: $\mathcal{G}(S_G(V_S, E_S), P_l, P_g, E_P, E_G) \leftarrow \mathbf{GSG}(\mathcal{D})$

GIG hidden layers:

for $l = 1:L$ do

GVU module: Locally and individually updating the graph edges $e_{n,m}^i \in E_S^i$, graph vertices $v_n^i \in V_S^i$, proxy edges $e_{n,p}^i \in E_P^i$ and local proxy vertices $P_l^i \in P_l$ in each GIG vertex S^i as: $\hat{\mathcal{G}}^l(\hat{S}_G(\hat{V}_S, \hat{E}_S), \hat{P}_l, P_g, \hat{E}_P, E_G) \leftarrow \mathbf{GVU}(\mathcal{G}^{l-1}(S_G(V_S, E_S), P_l, P_g, E_P, E_G))$

GGU module: Globally updating GIG edges $e^{i,j} \in E_G$ and global proxy vertices $P_g^i \in P_g$, and then pass global contexts to each GIG vertices by updating its proxy edges $e_{p,n}^i \in E_P^i$ and graph vertices $\hat{v}_n^i \in \hat{V}_S^i$ as: $\bar{\mathcal{G}}^l(\bar{S}_G(\bar{V}_S, \bar{E}_S), \hat{P}_l, \bar{P}_g, \bar{E}_P, \bar{E}_G) \leftarrow \mathbf{GGU}(\hat{\mathcal{G}}^l(\hat{S}_G(\hat{V}_S, \hat{E}_S), \hat{P}_l, P_g, \hat{E}_P, E_G))$

end for

GIG output layer: First applying the GVU module to individually update each GIG vertex, and then the GGU⁺ is employed to not only updates GIG edges, global proxy vertices and graph vertices in each GIG vertex but also additionally updates graph edges as: $\bar{\mathcal{G}}^L(\bar{S}_G(\bar{V}_S, \bar{E}_S), \hat{P}_l, \bar{P}_g, \bar{E}_P, \bar{E}_G) \leftarrow \mathbf{GGU}^+(\bar{\mathcal{G}}^L(\bar{S}_G(\bar{V}_S, \bar{E}_S), \hat{P}_l, P_g, \hat{E}_P, E_G))$

in Table 6 and 7, indicating that our approach is robust to not only different numbers of graph vertices connected to local/global proxy vertices but also different local proxy vertex initialisation strategies. In comparison to directly connect graph vertices contained in different GIG vertices, our proxy vertex and GIG edge-based strategy avoids the GIG sample to have extremely large number of edges to construct associations between GIG vertices. In summary, the GSG layer encodes the input data \mathcal{D} as an GIG sample $\mathcal{G}(S_G(V_S, E_S), P_l, P_g, E_P, E_G)$ (denoted as \mathcal{G} in the following sections).

4.2 GIG hidden layer

In the proposed GIG network, a set of GIG hidden layers are stacked after the GSG layer to learn downstream task-related features from the obtained GIG

Table 1: Notations for describing the initial GIG sample.

Notations	Descriptions
GIG sample	Graph-style data whose vertices can directly include graphs
GIG network/layer	Graph Neural Network (layer) that can process GIG samples
$\mathcal{G}(S_G, P_l, P_g, E_P, E_G)$	GIG sample
$S_G(V_S, E_S)$	the vertex/GIG vertex set of \mathcal{G}
$S^i(V_S^i, E_S^i)$	a vertex/GIG vertex in \mathcal{G}
V_S^i	the graph vertex set in GIG vertex S^i
v_n^i	a graph vertex in V_S^i
E_S^i	the graph edge set in GIG vertex S^i
$e_{n,m}^i$	a graph edge in E_S^i connecting v_n^i and v_m^i
P_l	the local proxy vertex set in \mathcal{G}
P_l^i	the local proxy vertex representing S^i
P_g	the global proxy vertex set in \mathcal{G}
P_g^i	the global proxy vertex of S^i collecting information from other GIG vertices S^j
E_P^i	the set of directed proxy edges for S^i
$e_{n,p_l}^i / e_{p_g,n}^i$	a pair directed proxy edges connecting v_n^i and P_l^i or P_g^i and v_n^i
E_G	the set of GIG edges in \mathcal{G}
$e_{i,j}$	a GIG edge in E_G connecting P_l^i and P_l^j

sample. Specifically, each GIG hidden layer consists of a **GVU module** which individually updates the graph contained in each GIG vertex based on its internal/local information, as well as a **GGU module** which enables the graphs contained in different GIG vertices to exchange their task-related cues. This allows each GIG hidden layer jointly models local information contained in each GIG vertex and relationships among GIG vertices, facilitating effective and global context-aware message exchanging during reasoning.

4.2.1 GIG Vertex Updating (GVU) module

Let the input to the GVU module be a GIG sample \mathcal{G} , it first independently updates the graph contained in each GIG vertex S^i , including its graph edges and graph vertices, and then passes such updated local cues to the corresponding local proxy vertex P_l^i via the updated directed proxy edges starting from a set of graph vertices v_n^i to P_l^i .

Locally updating graph edges and graph vertices: This module first updates each **graph edge feature** $e_{n,m}^i$ in a GIG vertex S^i by considering: (i) the $e_{n,m}^i$ itself; and (ii) the corresponding graph vertices v_n^i and v_m^i as:

$$\hat{e}_{n,m}^i = f_e^{\text{GVU}}(e_{n,m}^i, v_n^i, v_m^i) \quad (4)$$

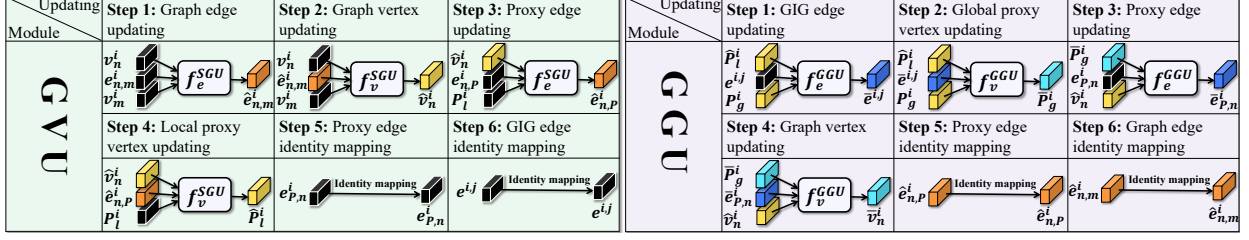


Fig. 3: Illustration of the propagation of the GVU and GGU module.

where f_e^{GVU} represents the graph edge feature updating function employed by the GVU. It then updates each **graph vertex feature** v_n^i by considering: (i) the graph vertex feature v_n^i ; (ii) v_n^i 's adjacent graph vertex features $v_m^i \in \mathcal{N}_{\text{local}}(v_n^i)$ in the corresponding GIG vertex \mathcal{S}^i ; and (iii) the updated graph edge $\hat{e}_{n,m}^i$ that connects v_n^i and its adjacent graph vertices $\mathcal{N}_{\text{local}}(v_n^i)$. This can be formulated as:

$$\hat{v}_n^i = f_v^{\text{GVU}}(v_n^i, \text{Agg}(g_v(\hat{e}_{n,m}^i, v_m^i) | v_m^i \in \mathcal{N}_{\text{local}}(v_n^i))) \quad (5)$$

where f_v^{GVU} is a differentiable vertex feature updating function in the GVU; g_v is a differentiable message passing function that passes the impact of each vertex feature to its neighbours; and Agg denotes an aggregation operation.

Locally updating proxy edges and local proxy vertices: Once all graph edges and graph vertices are updated, the GVU also updates each **directed proxy edge** e_{n,P_l}^i starting from each graph vertex v_n^i to its local proxy vertex P_l^i by considering: (i) the proxy edge e_{n,P_l}^i ; (ii) the corresponding updated graph vertices \hat{v}_n^i ; and (iii) the local proxy vertex P_l^i , which can be denoted as:

$$\hat{e}_{n,P_l}^i = f_e^{\text{GVU}}(e_{n,P_l}^i, \hat{v}_n^i, P_l^i) \quad (6)$$

where the f_e^{GVU} is re-employed as the proxy edge feature updating function. Finally, the **local proxy vertex** P_l^i is updated by aggregating messages passed from selected graph vertices (which are least similar to the local proxy vertex) through the corresponding updated directed proxy edges \hat{e}_{n,P_l}^i ($n = 1, 2, \dots, N_i$). This process can be formulated as:

$$\hat{P}_l^i = f_v^{\text{GVU}}(P_l^i, \text{Agg}(g_v(\hat{e}_{n,P_l}^i, \hat{v}_n^i))) \quad (7)$$

where f_v^{GVU} is re-employed as the local proxy vertex updating function. This way, each local proxy vertex \hat{P}_l^i summarises the locally updated graph information contained in its corresponding GIG vertex $\hat{\mathcal{S}}^i$. It should be emphasised that we follow previous GNNs [5, 73–76] to first update edges (e.g., graph edges / proxy edges), and then updates the corresponding vertices (graph vertices / local proxy vertices / global proxy vertices). Also, we found that first updating graph edges/vertices and then updating proxy edges/vertex lead to similar performances

as simultaneously updating them.

4.2.2 Global-level GIG Sample Updating (GGU) Module

After individually updating each GIG vertex, the GGU module aims to exchange messages among GIG vertices. It first passes locally updated cues from the local proxy vertex of each GIG vertex to the global proxy vertices of its adjacent GIG vertices, via the updated GIG edges. Then, the contextual information received in each global proxy vertex (i.e., containing cues passed from local proxy vertices of other GIG vertices) is further passed to its corresponding GIG vertex, enabling the contained graph to be updated based on contextual cues provided by graphs contained in other GIG vertices.

GIG edge and global proxy vertex updating: Given a directed GIG edge $e^{i,j} \in E_G$ starting from the locally updated local proxy vertices \hat{P}_l^i of the GIG vertex \mathcal{S}^i to the global proxy vertex P_g^j of the GIG vertex \mathcal{S}^j , the GGU updates it via a differentiable GIG edge updating function f_e^{GGU} as:

$$\bar{e}^{i,j} = f_e^{\text{GGU}}(e^{i,j}, \hat{P}_l^i, P_g^j) \quad (8)$$

Then, the GGU **exchanges messages among GIG vertices by updating their global proxy vertices** \hat{P}_g^i as \bar{P}_g^i based on: (i) the global proxy vertex feature P_g^i ; (ii) the local proxy vertices $\hat{P}_l^j \in \mathcal{N}_{\text{global}}(\hat{P}_g^i)$ ($j = 1, 2, \dots, I$ and $j \neq i$) of its neighbouring GIG vertices, which summarises the locally updated graphs in their corresponding GIG vertices; and (iii) the corresponding globally updated directed GIG edges $\bar{e}^{i,j}$ ($j = 1, 2, \dots, I$ and $j \neq i$) as:

$$\bar{P}_g^i = f_v^{\text{GGU}}(P_g^i, \text{Agg}(g_v(\bar{e}^{i,j}, \hat{P}_l^j) | \hat{P}_l^j \in \mathcal{N}_{\text{global}}(P_g^i))) \quad (9)$$

where f_v^{GGU} denotes a differentiable global proxy vertex feature updating function in the GGU. This way, each updated global proxy vertex would contain messages received from other locally updated GIG vertices, i.e., the updated global proxy vertices are global context-aware.

Globally updating proxy edges and graph vertices: Finally, the GGU passes the global contextual information received in each globally updated

global proxy vertex \bar{P}_g^i to the graph in the corresponding GIG vertex \mathcal{S}^i . This is achieved by first updating each **directed proxy edge feature** $e_{P_g,n}^i$ starting from \bar{P}_g^i to each of its connected graph vertex \hat{v}_n^i by considering: (i) the \bar{P}_g^i that contains messages received from other GIG vertices; (ii) the directed proxy edge $e_{P_g,n}^i$; and (iii) the locally updated graph vertex \hat{v}_n^i as:

$$\bar{e}_{P_g,n}^i = f_e^{\text{GGU}}(e_{P_g,n}^i, \bar{P}_g^i, \hat{v}_n^i) \quad (10)$$

where f_e^{GGU} is employed for updating directed proxy edges starting from global proxy vertices.

Then, the GGU updates graph vertex features that are connected with its global proxy vertex \bar{P}_g^i based on the global contextual information by considering: (i) each locally updated graph vertex \hat{v}_n^i that is connected with the global proxy vertex \bar{P}_g^i ; (ii) the globally updated global proxy vertex \bar{P}_g^i ; and (iii) the corresponding globally updated proxy edge $\bar{e}_{P_g,n}^i$ as:

$$\bar{v}_n^i = f_v^{\text{GGU}}(\hat{v}_n^i, \text{Agg}(g_v(\bar{e}_{P_g,n}^i, \bar{P}_g^i))) \quad (11)$$

where f_v^{GGU} updates these graph vertices based on the global contextual information encoded in the corresponding global proxy vertex. Since a GIG network would contain multiple GIG hidden layers, the global contextual information encoded in graph vertices that are connected with their global proxy vertices at the l_{th} hidden layer will be further utilized to update their related graph edges and the rest graph vertices by the GGU module at the $l + 1_{th}$ hidden layer or the GIG output layer. Therefore, the GGU module of each GIG hidden layer does not need to globally update graph edges and rest graph vertices.

4.3 GIG output layer

The GIG output layer has a similar architecture as the GIG hidden layer, which stacks a GGU module and a GGU⁺ module. Specifically, its GGU module individually updating each GIG vertex (i.e., locally updating graph edges and graph vertices of the graph) as well as its corresponding proxy edges and local proxy vertices based on the same functions defined by the GIG hidden layer. Then, the GGU⁺ module follows the same manner as the GGU module defined in the GIG hidden layer to first globally update GIG edges, global proxy vertices, proxy edges starting from global proxy vertices and graph vertices. In addition, it further updates each locally updated graph edge $\hat{e}_{n,m}^i$ as $\bar{e}_{n,m}^i$ in each GIG vertex by considering: (i) the $\hat{e}_{n,m}^i$ itself; and (ii) the corresponding globally updated graph vertices \bar{v}_n^i and \bar{v}_m^i as:

$$\bar{e}_{n,m}^i = f_e^{\text{GVU}}(\hat{e}_{n,m}^i, \bar{v}_n^i, \bar{v}_m^i) \quad (12)$$

where f_e^{GVU} is re-employed. Subsequently, the graph vertices that are not connected with global proxy vertices are also updated based on these globally updated graph vertices \bar{v}_n^i and \bar{v}_m^i as well as other globally updated graph vertices (i.e., graph vertices connected with global proxy vertices) under the same rule of Eqn. 5. This way, all graph vertices and graph edges of graphs contained in the final output GIG sample are locally and globally updated. Note that our GIG network allows for flexible customization of its edge and vertex updating functions from existing GNNs (e.g., GatedGCN [39] and GAT [38]) and thus it can jointly handle graphs with varying typologies and multi-dimensional edge graphs. To keep a simple form, this paper maintains a consistent function for all edges' updating (i.e., f_e^{GVU} and f_e^{GGU} have the same form), as well as the same vertex updating function for all types of vertices' updating (i.e., f_v^{GVU} and f_v^{GGU} are the same).

4.4 Model complexity analysis

The GIG network consists of a GSG layer, a set of GIG hidden layers and a GIG output layer. Specifically, **the GSG layer** defines each local proxy vertex through averaging all graph vertex features of the corresponding GIG vertex. The averaging calculation for each GIG vertex consists of one summation operation and one division operation. The summation operation requires $O(n)$ and division operation requires $O(1)$. Then the time complexity for local proxy vertex generation procedure can be defined as $O(|\mathcal{G}| \times n)$. In this paper, the generation of proxy-edges are totally based on the cosine similarity between graph vertices and their corresponding local/global proxy vertex, which is defined as:

$$\begin{aligned} \text{CosSim}(P_l^i, v_n^i) &= \frac{P_l^i \cdot v_n^i}{\|P_l^i\| \|v_n^i\|} \\ &= \frac{\sum_{i=1}^n P_{l,i}^i v_{n,i}^i}{\sqrt{\sum_{i=1}^n P_{l,i}^i{}^2} \sqrt{\sum_{i=1}^n v_{n,i}^i{}^2}} \quad (13) \end{aligned}$$

where P_l^i represents a local proxy vertex feature and v_n^i represents one of its graph vertex feature, i.e., $P_{l,i}^i$ and $v_{n,i}^i$ denote the i_{th} element in P_l^i and v_n^i , respectively. Specifically, this calculation process involves three steps: (i) Dot Product calculation: The dot product $P_l^i \cdot v_n^i$ necessitates n multiplication operations (one for each pair of corresponding elements from vectors P_l^i and v_n^i) and $n - 1$ addition operations to sum these products. Hence, the time complexity for computing the dot product is $O(n)$; (ii) Norm calculation: The norm of a vector, $\|P_l^i\|$ or $\|v_n^i\|$, requires n squaring operations, $n - 1$ addition operations to aggregate these squares, and a square root operation. Since both vectors undergo this process, the complexity remains $O(n)$ for each

norm calculation; and (iii) Division operation: dividing the dot product by the product of the norms involves a single division operation, which is considered as $O(1)$ in complexity. In summary, the overall time complexity for computing the cosine similarity between two n -dimensional vectors is $O(n)$. Continuously, the main operation in proxy edge generation is to calculate the cosine similarity between local proxy vertex and graph vertices in each GIG vertex. Since the numbers of graph vertices in different GIG vertices could be different, they can be represented as $V_S = \{|V_S^1|, |V_S^2|, |V_S^3|, \dots, |V_S^N|\}$. Consequently, the time complexity of proxy edge generation procedure can be defined as $O(|\mathcal{G}| \times \max(V_S) \times n)$, where $|\mathcal{G}|$ represents the number of GIG vertices in the GIG sample. Then, the connections (GIG edges) between global proxy vertices and local proxy vertices from other GIG vertices are defined by computing self-cosine similarity on the matrix consisted of $|\mathcal{G}|$ local proxy vertex features (GSG module only works before training, while the global proxy vertex features are set as zero vectors here), resulting in the time complexity of $O(|\mathcal{G}|^2 \times n)$. Consequently, the overall time complexity of the GSG module is $O(|\mathcal{G}| \times \max(V_S) \times n + |\mathcal{G}|^2 \times n)$. *The GSG module will only be called once before the starting of training to generate the GIG sample.* Then, each **GIG hidden layer** is made up of a GVU and a GGU module, whose exact time complexity is determined by the edge/vertex updating algorithms chosen here. Assuming that the total time complexity of the GVU and GGU are $O(f_1)$ and $O(f_2)$, respectively, the time complexity of each GIG hidden layer can be defined as $O(f_1 + f_2)$. Finally, **GIG output layer** additionally updates graph vertices that are not connected with global proxy vertices as well as graph edges compared to GIG hidden layer, whose time complexity can be denoted as $O(f_3)$ and $O(f_4)$. As a result, the total time complexity of each GIG output layer can be defined as $O(f_1 + f_2 + f_3 + f_4)$. The time complexity analysis of example GIG-GatedGCN and GIG-GAT, practical time consumption of our GIG network and the influence of the numbers of proxy edges and GIG edges on the GVU and GGU’s complexity are provided in the Supplementary Material.

5 Experiment

This section comprehensively evaluates our GIG on 14 different datasets (explained in Sec. 5.1), where the implementation details and evaluation metrics are detailed in Sec. 5.2. We show that our GIG-GNNs which represent each vertex as a graph are superior to existing GNNs that represent each vertex as a vector/single value in Sec. 5.3. Finally, Sec. 5.4 comprehensively evaluate various aspects of our GIG in terms of both effectiveness and efficiency.

5.1 Datasets

This paper evaluate our approach on 14 graph and non-graph datasets. Firstly, **12 benchmark graph datasets** are employed to evaluate the performance of the proposed GIG network on **generic graph analysis**, including (i) MNIST [77] and CIFAR10 [78] image classification datasets (i.e., their images are converted into graphs by a widely-used graph benchmark [37]), three TU datasets [79–81], and the OGBG-PPA biological graph dataset (describing protein-protein associations) dataset for graph classification; (ii) ZINC [82], ZINC-full [82] and AQSOL [83] molecular graph datasets for graph regression; (iii) PATTERN node-level graph pattern recognition [37] and CLUSTER semi-supervised graph clustering [37] datasets for node (vertex) classification; and (iv) TSP city route plan dataset [84] for the link prediction. Then, our GIG is evaluated on **two non-graph real-world multi-graph datasets**, i.e., two subsets of the NTU RGB+D human skeleton video-based action recognition dataset which contains 56,880 skeleton action clips belonging to 60 classes (performed by 40 different participants). Here, each clip is recorded through three Microsoft Kinect v2 cameras at horizontal angles of 45° , 0° , -45° , and contains human actions performed by one or two subjects. The employed two subsets are: (i) Cross-Subject (X-Sub) dataset, where clips of 20 subjects are used for training, and clips of the remaining 20 subjects are used for validation; and (ii) Cross-View (X-View) dataset, where two of the three camera-views are utilized for training, and the other is utilized for validation.

5.2 Implementation details

To demonstrate the effectiveness of our GIG network, we apply it to 14 datasets for 5 different tasks, where different vertex and edge updating algorithms inherited from GNNs are employed. Detailed training settings (e.g., hyper-parameter settings) are provided in the Supplementary Material.

Experiments on graph datasets: We individually apply the vertex/edge updating mechanisms of the widely-used GatedGCN (the default setting), GAT and GCN implemented by [37], as well as the DeeperGCN [85] to construct our GIG network for generic graph analysis experiments. Here, a batch of input graph samples are combined as a GIG sample by the GSG layer, where each GIG vertex includes a graph sample. The initial feature of each local proxy vertex is obtained through averaging all of its graph vertex features, while the initial feature of each global proxy vertex/proxy edge is set as a zero vector. Then, we customize the edge/vertex updating functions of GVU and GGU modules based on the GatedGCN, GAT, GCN and DeeperGCN, respectively. During training, we follow the same training settings (e.g.,

loss functions, hyper-parameters, and AdamW optimizer []) as the benchmarking [37] and DeeperGCN. The detailed evaluation metrics for these generic graph analysis tasks are: (i) graph classification results on MNIST [77], TUs [37] and CIFAR10 [78] datasets are measured by classification accuracy; (ii) graph regression results on ZINC, ZINC-full [82] and AQSOL [83] datasets are measured by Mean Absolute Error (MAE); (iii) node (vertex) classification results on PATTERN [37] and CLUSTER [37] are measured by classification accuracy; (iv) link prediction results on TSP [84] and OGBG-PPA [86] are measured by F1-score and classification accuracy, respectively.

Experiments on human skeleton video-based action recognition datasets: This paper additionally customize our GIG based on the edge/node updating algorithms of the state-of-the-art CTR-GCN [63] and widely-used ST-GCN [16], resulting in GIG-CTR-GCN and GIG-ST-GCN models for human skeleton video-based action recognition task. Here, each human skeleton video is encoded as a GIG sample by the GSG layer, where each skeleton frame is described as a graph contained in a GIG vertex while initial local/global proxy vertices and proxy edges are defined following the same rule described above. For fair comparison, we follow the same training settings as the original ST-GCN and CTR-GCN, and the evaluation metrics is the Top-1 classification accuracy.

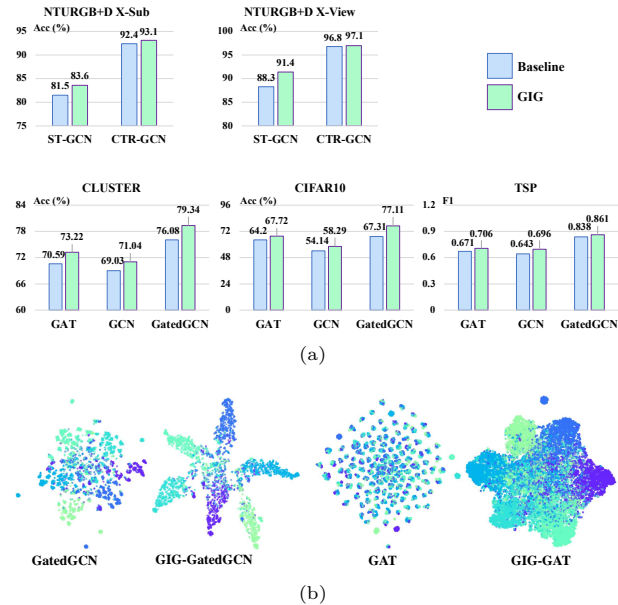


Fig. 4: (a) Comparison between original GNNs and GIG-GNNs with the same vertex/edge updating functions; (b) t-SNE visualisation of features learned on CLUSTER dataset (a six classes vertex classification dataset), where each dot represents a vertex and each colour represents a category label.

5.3 Comparison with state-of-the-art methods

This section compares our GIG network with existing approaches on various tasks. Fig. 4(a) first validates that our GIG network is flexible to be customized by edge/vertex updating strategies defined by various existing GNNs. Importantly, *with the same edge/vertex updating strategies, our graph vertex-based GIG consistently achieved performance gains over existing vector vertex-based GNNs for all evaluated tasks.* Besides, Fig. 4(b) demonstrates that representations learned by our GIG networks are more discriminative than baseline GNNs that have the same edge/vertex updating functions. This indicates that relationships among graph samples encoded by our GIG can provide complementary and task-specific cues for generic graph analysis, as well as representing and processing multiple objects (graphs) in multi-graph data samples.

5.3.1 Evaluation on NTU RGB+D datasets

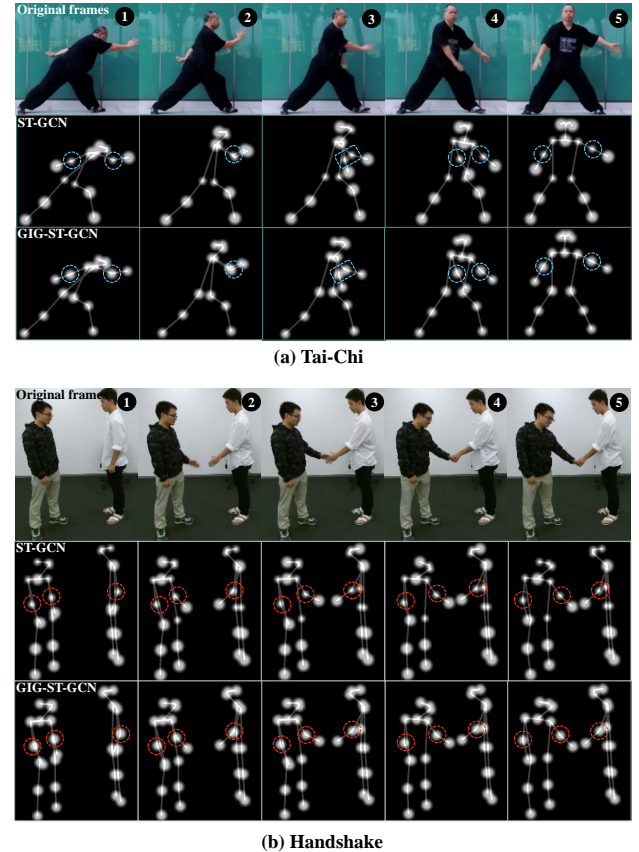


Fig. 5: Visualization of features learned by GIG-ST-GCN and ST-GCN, where sizes of white circles represent their importance for action recognition defined by networks. GIG-ST-GCN paid similar attentions to all joints throughout all frames with more attentions to crucial joints than ST-GCN.

Table 2: Experimental results on 11 benchmark datasets from [37]. Bolder results denote the best performance. Unfilled cells denote that these publications haven’t evaluated their methods on the corresponding datasets.

Task	Graph classification				
Dataset	MNIST	CIFAR10	ENZYMES	DD	PROTEINS
Method	Acc(%) \uparrow				
GCN[31]	90.12 \pm 0.15	54.14 \pm 0.39	65.833 \pm 4.610	72.758 \pm 4.083	76.098 \pm 2.406
GIN[87]	96.49 \pm 0.25	55.26 \pm 1.53	65.333 \pm 6.823	71.910 \pm 3.873	74.117 \pm 3.357
δ -2-GNN[88]	-	-	-	-	-
δ -2-LGNN[88]	-	-	-	-	-
GAT[38]	95.54 \pm 0.21	64.22 \pm 0.46	68.500 \pm 5.241	75.900 \pm 3.824	76.277 \pm 2.410
GatedGCN[39]	97.34 \pm 0.14	67.31 \pm 0.31	65.667 \pm 4.899	72.918 \pm 2.090	76.363 \pm 2.904
PNA[89]	97.94 \pm 0.12	70.86 \pm 0.27	-	-	-
DGN[90]	-	72.84 \pm 0.42	-	-	-
EGT[91]	98.17 \pm 0.09	68.70 \pm 0.41	-	-	-
ARGNP[92]	-	73.90 \pm 0.15	-	-	-
EXPHORMER[93]	98.55 \pm 0.04	74.69 \pm 0.13	-	-	-
GNAS-MP[94]	98.01 \pm 0.10	70.10 \pm 0.44	-	-	-
GIG-GatedGCN	98.80 \pm 0.03	77.11 \pm 0.05	80.25 \pm 2.770	89.09 \pm 3.151	85.12 \pm 1.982

Graph regression			Node classification		Edge classification
ZINC(10K)	ZINC-full	AQSOL	PATTERN	CLUSTER	TSP
	MAE \downarrow		Acc(%) \uparrow		F1 \uparrow
0.113 \pm 0.002	0.278 \pm 0.003	1.333 \pm 0.013	85.61 \pm 0.03	69.03 \pm 1.37	0.643 \pm 0.001
0.088 \pm 0.002	0.387 \pm 0.015	1.894 \pm 0.024	85.59 \pm 0.01	64.72 \pm 1.55	0.656 \pm 0.003
-	0.042 \pm 0.003	-	-	-	-
-	0.045 \pm 0.006	-	-	-	-
0.111 \pm 0.002	0.384 \pm 0.007	1.403 \pm 0.008	78.27 \pm 0.19	70.59 \pm 0.45	0.671 \pm 0.002
0.214 \pm 0.013	-	0.996 \pm 0.008	85.57 \pm 0.09	73.84 \pm 0.33	0.838 \pm 0.002
-	-	-	86.57 \pm 0.08	-	-
-	-	-	86.68 \pm 0.03	-	-
0.108 \pm 0.009	-	-	86.82 \pm 0.02	79.23 \pm 0.35	0.853 \pm 0.001
0.136 \pm 0.002	-	-	-	77.35 \pm 0.05	0.855 \pm 0.001
-	-	-	86.74 \pm 0.02	78.07 \pm 0.04	-
0.242	-	-	86.80 \pm 0.10	62.21 \pm 0.20	-
0.125 \pm 0.001	0.029 \pm 0.001	0.927 \pm 0.018	86.87 \pm 0.01	79.34 \pm 0.03	0.863 \pm 0.001

Table 3: Results on two human skeleton video-based action recognition datasets. Bolder denotes the best performance.

Dataset	X-Sub	X-View
	Acc(%)	
ST-GCN[16]	81.5	88.3
AS-GCN[95]	86.8	94.2
SGN[96]	89.0	94.5
DGNN[41]	89.9	96.1
ST-TR-agcn[97]	90.3	96.3
shift-GCN[98]	90.7	96.5
DC-GCN+ADG[99]	90.8	96.6
Dynamic GCN[100]	91.5	96.0
MS-G3D[101]	91.5	96.2
MST-GCN[102]	91.5	96.6
CTR-GCN(4-ensemble)[63]	92.4	96.8
InfoGCN(4-ensemble)[103]	92.7	96.9
HD-GCN(4-ensemble)[104]	93.0	97.0
GIG-ST-GCN	83.6	91.4
GIG-CTR-GCN(4-ensemble)	93.1	97.1

Table 3 evaluate our GIG on skeleton video (multi-graph data sample)-based action recognition task. Although the advanced CTR-GCN already achieved classification accuracy of 92.4% and 96.8%

on X-Sub and X-View datasets, incorporating its vertex and edge updating strategies into our GIG network results in significant (refer to the Supplementary Material for statistical difference analysis) and consistent improvements of 0.8% and 0.3% on X-Sub and X-View datasets, respectively. Specifically, GIG-ST-GCN outperformed the original ST-GCN with more than 2.5% and 3.5% improvements on two datasets, while GIG-CTR-GCN achieved the state-of-the-art performance on both datasets, despite that all competitors were specifically designed for skeleton-based action recognition task while the GIG is a generic GNN that accommodates various tasks. Fig. 5 highlights the superiority of GIG-ST-GCN over ST-GCN in paying relatively similar attentions to all joints throughout all frames, with greater attention paid to crucial joints (e.g., elbows). In contrast, the original ST-GCN focuses on less important joints (e.g., lower limbs which remained almost still in the action) and ignores crucial joints (e.g., joints moved in the next frame). This indicates our GIG network’s ability in exchanging information between GIG vertices (skeleton frames), which considers each human

action as a whole-body movements, thereby learned more effective representations.

Table 4: Experimental results on OGBG-PPA large-scale datasets from [79]. Bolder results denote the best performance.

Datasets Models	OGBG-PPA Acc(%)
GPS [105]	0.8015
ExpC [106]	0.7976
DeeperGCN+FLAG [107]	0.7752
DeeperGCN [85]	0.7712
GIG-DeeperGCN	0.8017

5.3.2 Evaluation on generic graph analysis datasets

Table 2 and 4 compares our GIG with widely-used GNNs on all typical graph analysis tasks (graph/vertex/edge-level analysis), which highlights the following observations: **(i)** GIG achieved state-of-the-art performances on 11/12 datasets, demonstrating its scalability and effectiveness for various graph analysis tasks. While GIG ranked second on the ZINC(10K) dataset, it still largely improves its baseline GatedGCN from 0.214 to 0.125. However, on the ZINC-full dataset that has the same distribution as ZINC(10k) but larger number of samples, our GIG reached out the state-of-the-art results, suggesting the small number of training samples in ZINC(10K) limited the performance of our GIG; **(ii)** Comparing GIG-GatedGCN with GatedGCN, we found that our GIG-GatedGCN obtained more than 10% average improvement on all datasets. This directly confirms the effectiveness of GIG vertex communication in the proposed GIG, which also maintains the superiority of GatedGCN; and **(iii)** our GIG outperforms GNAS-MP that employs Neural Architecture Search (NAS) to explore task-specific weights and optimal architecture, showing that GIG can potentially advance the state-of-the-art performance on this benchmark using more advanced vertex/edge updating strategies.

5.4 Ablation Studies

The default vertex/edge updating strategies for generic graph analysis and action recognition ablation experiments are inherited from GatedGCN and ST-GCN, respectively.

5.4.1 Impacts of individual modules

Table 5 indicates that the variant V5, which integrated both GVU and GGU on V2, achieved the highest performance on all tasks, especially better than V1. Here, V1 refers to the system that treats each GIG vertex in a GIG sample as a vector, which

Table 5: Ablation results achieved by **V1**: treating each GIG vertex of the GIG sample as a vector; **V2**: combining all GIG vertices as a large graph; **V3**: using GVU only; **V4**: using GGU only; and **V5**: the full GIG network.

	Modules			Datasets		
	GSG	GVU	GGU	MNIST Acc(%)	TSP F_1	NTU X-Sub Acc(%)
V1	✗	✗	✗	26.32 ± 0.01	–	13.4
V2	✓	✗	✗	94.75 ± 0.01	0.853 ± 0.001	76.3
V3	✓	✗	✓	96.42 ± 0.03	0.567 ± 0.006	57.0
V4	✓	✓	✗	97.32 ± 0.08	0.835 ± 0.003	81.5
V5	✓	✓	✓	98.80 ± 0.03	0.863 ± 0.001	83.6

is obtained by averaging all graph vertex features in the corresponding GIG vertex, (i.e., a skeleton frame or a graph sample). This finding suggests that *graphs are better vertex representations than vectors for various types of data*. Furthermore, the GVU contributes significantly to the final performance, as evidenced by the improved performance of V5 compared to V3. The results that V5 outperformed V4 also indicate that the GIG network can better model temporal correlations among GIG vertices derived from human action clips, as well as underlying relationship cues among multiple graph samples, thus providing more discriminative information for both action recognition and generic graph analysis tasks. Finally, V5 outperformed V2 which treat all local/global proxy vertices and graph vertices as standard graph vertices, and all edges as standard graph edges, i.e., all vertices are simultaneously processed using GatedGCN/ST-GCN, validated the superiority of our local-global updating strategy (GGU and GVU).

5.4.2 Impacts of proxy edge number

Table 6: Ablation study for different proxy edge numbers.

Datasets	MNIST	PATTERN	TSP
Proportion	Test Acc(%) ↑	Test Acc(%) ↑	Test F_1 ↑
10%	98.80 ± 0.03	86.87 ± 0.01	0.863 ± 0.001
40%	98.72 ± 0.04	86.83 ± 0.02	0.859 ± 0.001
70%	98.61 ± 0.07	86.80 ± 0.05	0.860 ± 0.003
100%	98.71 ± 0.05	86.72 ± 0.02	0.857 ± 0.006

Table 6 presents the results achieved by connecting each local/global proxy vertex with different proportions of graph vertices, showing that the performance of our GIG is robust to this variable, where the best performance is achieved when each local/global proxy vertex connects 10% of its graph vertices.

Table 7: Results achieved by different settings.

Dataset	MNIST	PATTERN	TSP
# GIG layers	Test Acc(%) \uparrow		Test F_1 \uparrow
1	97.82 \pm 0.02	86.79 \pm 0.01	0.842 \pm 0.001
2	98.50 \pm 0.04	86.87 \pm 0.01	0.858 \pm 0.001
3	98.80 \pm 0.03	86.79 \pm 0.01	0.863 \pm 0.001
Proxy edge def.	Test Acc(%) \uparrow		Test F_1 \uparrow
Proxy edge def. (i)	98.80 \pm 0.03	86.87 \pm 0.01	0.863 \pm 0.001
Proxy edge def. (ii)	98.72 \pm 0.04	86.83 \pm 0.02	0.859 \pm 0.001
Proxy edge def. (iii)	98.61 \pm 0.07	86.80 \pm 0.05	0.860 \pm 0.003
Proxy edge def. (iv)	98.71 \pm 0.05	86.72 \pm 0.02	0.857 \pm 0.006
GIG edge def.	Test Acc(%) \uparrow		Test F_1 \uparrow
GIG edge def. (i)	98.76 \pm 0.05	86.82 \pm 0.03	0.861 \pm 0.005
GIG edge def. (ii)	98.78 \pm 0.04	86.85 \pm 0.02	0.859 \pm 0.001
GIG edge def. (iii)	98.80 \pm 0.03	86.87 \pm 0.01	0.863 \pm 0.001
Proxy vertex init.	Test Acc(%) \uparrow		Test F_1 \uparrow
Random graph vertex	98.72 \pm 0.02	86.84 \pm 0.01	0.857 \pm 0.001
Largest L2 norm	98.60 \pm 0.03	86.49 \pm 0.02	0.781 \pm 0.001
Smallest L2 norm	98.59 \pm 0.03	86.48 \pm 0.01	0.830 \pm 0.001
Avg. graph vertices	98.80 \pm 0.03	86.87 \pm 0.01	0.863 \pm 0.001

5.4.3 Impacts of different proxy edge connection strategies

Table 7 presents the comparison among different proxy edge connection strategies: (i) connecting directed proxy edges from graph vertices that are **least similar** to each local proxy vertex to it, and each global proxy vertex to graph vertices that are **most similar** to the corresponding local proxy vertex; (ii) connecting directed proxy edges from graph vertices that are **least similar** to each local proxy vertex to it, and each global proxy vertex to graph vertices that are **least similar** to the corresponding local proxy vertex; (iii) connecting directed proxy edges from graph vertices that are **most similar** to each local proxy vertex to it, and each global proxy vertex to graph vertices that are **least similar** to the corresponding local proxy vertex; and (iv) connecting directed proxy edges from graph vertices that are **most similar** to each local proxy vertex to it, and each global proxy vertex to graph vertices that are **least similar** to the corresponding local proxy vertex. Although there are very small performance variations, the strategy (i) achieved the best performance, which has been utilized in this paper. Further visualization results and analysis can be found in the Supplementary Material. *Note that the generation of proxy edge are only achieved in the GSG module, where every global proxy vertex will be set as zero vector. Then, the similarity calculation mentioned above will actually build on the feature of local proxy vertex.*

5.4.4 Impacts of different GIG edge connection strategies

Table 7 also compares different GIG edge connection strategies: (i) connecting bidirectional directed edges from each global proxy vertex to local proxy vertices that are **most similar** to it; (ii) connecting bidirectional directed edges from each global proxy vertex to local proxy vertices that are **least similar** to it;

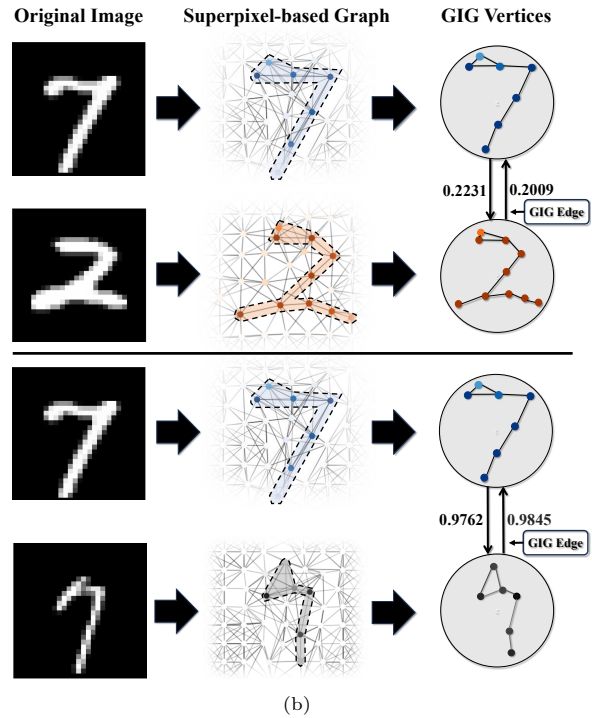
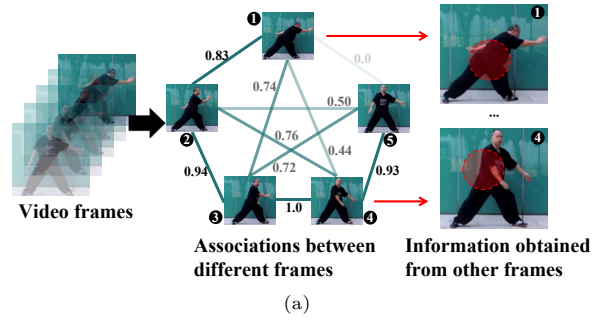


Fig. 6: Visualization of: (a) GIG edges constructed for the action recognition tasks; and (b) GIG edges constructed for generic graph analysis tasks.

and (iii) half of bidirectional directed edges are connected from each global proxy vertex to local proxy vertices that are most similar to it, while the rest bidirectional directed edges are connected from each global proxy vertex to local proxy vertices that are **least similar** to it. Here, we found that the strategy (iii) outperformed other strategies, which is the default setting adopted in the paper. Such results again show that our GIG is robust to this variable. We also illustrate the characteristics of the initial GIG edges learned for skeleton-based action recognition in Figure 6(a), where each connects a pair of GIG vertices (frames). It can be seen that the GIG edges connecting similar frames (i.e., greater temporal proximity) are typically represented by larger weights. Besides, Figure 6(b) further visualizes that GIG edges learned between GIG vertices containing two hand-written numbers (described by superpixel-based graphs/GIG vertices [37]) are associated with their similarity. These suggest that the learned GIG

edges can partially represent correlations between GIG vertices.

5.4.5 Effects of the number of stacked GIG hidden layers

Table 7 demonstrates the robustness of our GIG in terms of the number of GIG layers it contains. Although the optimal number of layers and input samples varied across datasets, the performances remains relatively stable, with less than 0.1% variation on vertex classification task when stacking three different numbers of GIG layers. Although even shallow GIG networks outperformed existing deep GNNs (e.g., 2 or 3 layer-GIG outperformed 16 layer-GatedGCN on PATTERN, CLUSTER and TSP), the complexity of GIG networks are practically not more than existing GNNs with the same edge/vertex updating functions (discussed in 4.4 and the section named Runtime Analysis in Supplementary Material). Here, one-layer GIG-ST-GCN and GIG-CTR-GCN are used for human skeleton-based action recognition, following their original proposals.

5.4.6 Effects of different local proxy vertex initialization strategies

Table 7 indicates that while the initializing each local proxy vertex by averaging all of its graph vertices yielded highest performances across all three tasks, the differences for four initialization methods were negligible. These suggest that the GSG layer can maintain robust performances across different local proxy vertex initialization methods.

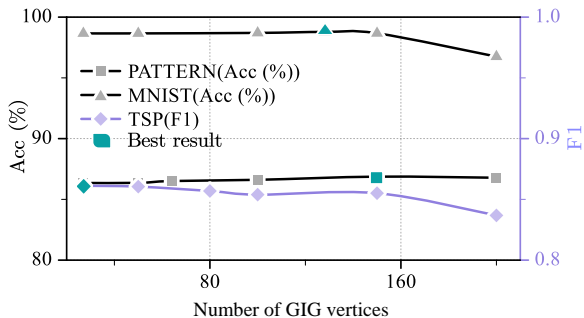


Fig. 7: Results achieved for GIG samples consisting of different numbers of GIG vertices.

5.4.7 Effects of the GIG vertex number in each GIG sample.

Figure 7 illustrates the capability of our GIG network in simultaneously handling different numbers of input graph samples for generic graph analysis, which shows that its performances remain stable or slightly varied when the number of input graph samples varies from 27 to 200 on all tasks. This highlights that the

potential of the proposed GIG network for real-world applications that require jointly analysing different numbers of graphs.

Table 8: Results achieved for GIG layers with varying arrangements of stacking GGU and GVU modules.

Datasets Variants	MNIST Acc(%)	TSP F_1	NTU X-Sub Acc(%)
GGU \rightarrow GVU	98.59 \pm 0.02	0.855 \pm 0.001	57.1
GVU \rightarrow GGU	98.80 \pm 0.03	0.863 \pm 0.001	83.6

5.4.8 Effects of GVU and GGU’s order in GIG layers.

Table 8 presents a comparison between two variants of the GIG layer, namely locally updating first (i.e., GVU module is placed at the first) and globally updating first (i.e., GGU module is placed at the first). The results demonstrate that the order of updating local and global information has little impact on the performances for the generic graph analysis tasks where no temporal correlations among GIG vertices.

6 Conclusion and discussion

This paper proposes a novel GIG network which can process graph-style data (i.e., GIG sample) whose vertices are represented by graphs rather than vectors or single values, allowing to effectively analyze real-world multi-graph data or a batch of graph samples. It also provides flexibility in vertex / edge updating functions by allowing customization from existing GNNs. Experimental results show that: (i) our GIG achieved the state-of-the-art performances on 13 out of 14 benchmark datasets corresponding to different tasks; (ii) our approach is robust to all of its main variables (e.g., proxy edge connection strategies, GIG edge connection strategies, proxy vertex initialization strategies, the number of GIG hidden layers, etc.), validating and emphasizing its generalization capability, i.e., our GIG is easy to be deployed; (iii) the proposed GVU and GGU modules can effectively learn task-related and complementary cues from each graph as well as the relationships among graphs; (iv) Connecting more graph vertices for each local proxy vertex, including more GIG vertices for each global proxy vertex, or adding more GIG layers did not guarantee an absolute improvement in performance, suggesting that the performance of GIG is largely independent to its complexity; and (v) the performance of GIG is basically robust when the order of GVU and GGU is changed.

The main limitation of our approach is that its GSG layer requires an additional task/data-dependent graph representation transformation step

to convert multiple non-graph frames/objects contained in real-world data samples into a set of GIG vertices. Besides, the superior performance of our model is at the cost of its relatively high computational complexity despite that practically its runtime is not clearly higher than standard GNNs. As a result, our future work will focus on not only developing an effective and generic graph representation learning module to replace the additional task/data-dependent graph representation transformation step/reducing the model complexity, but also evaluating our GIG on more related tasks/data.

Data Availability Statement. The authors affirm that the data supporting the findings of this study are openly accessible at GitHub project <https://github.com/graphdeeplearning/benchmarking-gnns> for MNIST, CIFAR10, DD, PROTEINS, ENZYMES, ZINC-10K, ZINC-full, AQSOL, PATTERN, CLUSTER, and TSP, at <https://ogb.stanford.edu/docs/graphprop/> for OGBG-PPA, and at <https://rose1.ntu.edu.sg/dataset/actionRecognition> for NTU RGB+D. Our code can be accessed at <https://github.com/wangjs96/Graph-in-Graph-Neural-Network>.

References

- [1] West, D.B., *et al.*: Introduction to Graph Theory vol. 2. Prentice hall Upper Saddle River, Upper Saddle River (2001)
- [2] Ying, C., Cai, T., Luo, S., Zheng, S., Ke, G., He, D., Shen, Y., Liu, T.: Do transformers really perform bad for graph representation? arXiv 2021. arXiv preprint arXiv:2106.05234
- [3] Satorras, V.G., Hoogeboom, E., Welling, M.: E (n) equivariant graph neural networks. In: International Conference on Machine Learning, pp. 9323–9332 (2021). PMLR
- [4] Frasca, F., Rossi, E., Eynard, D., Chamberlain, B., Bronstein, M., Monti, F.: Sign: Scalable inception graph neural networks. arXiv preprint arXiv:2004.11198 (2020)
- [5] Bresson, X., Laurent, T.: Residual gated graph convnets. arXiv preprint arXiv:1711.07553 (2017)
- [6] Hamilton, W.L.: Graph Representation Learning. Morgan & Claypool Publishers, San Rafael (2020)
- [7] Pareja, A., Domeniconi, G., Chen, J., Ma, T., Suzumura, T., Kanezashi, H., Kaler, T., Schardl, T., Leiserson, C.: Evolvegc: Evolving graph convolutional networks for dynamic graphs. In: Proceedings of the AAAI Conference on Artificial Intelligence, vol. 34, pp. 5363–5370 (2020)
- [8] Song, Y., Luo, C., Jackson, A., Jia, X., Xie, W., Shen, L., Gunes, H., Song, S.: Merg: Multi-dimensional edge representation generation layer for graph neural networks. In: ICASSP 2024-2024 IEEE International Conference on Acoustics, Speech and Signal Processing (ICASSP), pp. 5475–5479 (2024). IEEE
- [9] Yang, K., Swanson, K., Jin, W., Coley, C., Eiden, P., Gao, H., Guzman-Perez, A., Hopper, T., Kelley, B., Mathea, M., *et al.*: Analyzing learned molecular representations for property prediction. Journal of chemical information and modeling **59**(8), 3370–3388 (2019)
- [10] He, X., Deng, K., Wang, X., Li, Y., Zhang, Y., Wang, M.: Lightgcn: Simplifying and powering graph convolution network for recommendation. In: Proceedings of the 43rd International ACM SIGIR Conference on Research and Development in Information Retrieval, pp. 639–648 (2020)
- [11] Liu, X., Meng, S., Li, Q., Qi, L., Xu, X., Dou, W., Zhang, X.: Smef: Social-aware multi-dimensional edge features-based graph representation learning for recommendation. In: Proceedings of the 32nd ACM International Conference on Information and Knowledge Management, pp. 1566–1575 (2023)
- [12] Brissman, E., Johnander, J., Danelljan, M., Felsberg, M.: Recurrent graph neural networks for video instance segmentation. International Journal of Computer Vision **131**(2), 471–495 (2023)
- [13] Wang, S., Wang, Z., Li, H., Chang, J., Ouyang, W., Tian, Q.: Accurate fine-grained object recognition with structure-driven relation graph networks. International Journal of Computer Vision **132**(1), 137–160 (2024)
- [14] Wu, Z., Lu, J., Han, J., Bai, L., Zhang, Y., Zhao, Z., Song, S.: Domain separation graph neural networks for saliency object ranking. In: Proceedings of the IEEE/CVF Conference on Computer Vision and Pattern Recognition, pp. 3964–3974 (2024)
- [15] Deng, B., Song, S., French, A.P., Schluppeck, D., Pound, M.P.: Advancing saliency ranking with human fixations: Dataset models and benchmarks. In: Proceedings of the IEEE/CVF Conference on Computer Vision and Pattern Recognition, pp. 28348–28357 (2024)

- [16] Yan, S., Xiong, Y., Lin, D.: Spatial temporal graph convolutional networks for skeleton-based action recognition. In: AAAI (2018)
- [17] Song, S., Song, Y., Luo, C., Song, Z., Kuzucu, S., Jia, X., Guo, Z., Xie, W., Shen, L., Gunes, H.: Gratis: Deep learning graph representation with task-specific topology and multi-dimensional edge features. arXiv preprint arXiv:2211.12482 (2022)
- [18] Ma, C., Yang, F., Li, Y., Jia, H., Xie, X., Gao, W.: Deep human-interaction and association by graph-based learning for multiple object tracking in the wild. *International Journal of Computer Vision* **129**, 1993–2010 (2021)
- [19] Tu, J., Wu, G., Wang, L.: Dual graph networks for pose estimation in crowded scenes. *International Journal of Computer Vision* **132**(3), 633–653 (2024)
- [20] Qiao, M., Liu, Y., Xu, M., Deng, X., Li, B., Hu, W., Borji, A.: Joint learning of audio–visual saliency prediction and sound source localization on multi-face videos. *International Journal of Computer Vision*, 1–23 (2023)
- [21] Song, S., Shao, Z., Jaiswal, S., Shen, L., Valstar, M., Gunes, H.: Learning person-specific cognition from facial reactions for automatic personality recognition. *IEEE Transactions on Affective Computing* **14**(4), 3048–3065 (2022)
- [22] Xu, J., Gunes, H., Kusumam, K., Valstar, M., Song, S.: Two-stage temporal modelling framework for video-based depression recognition using graph representation. *IEEE Transactions on Affective Computing* (2024)
- [23] Perona, P., Malik, J.: Scale-space and edge detection using anisotropic diffusion. *TPAMI* (1990)
- [24] Battaglia, P., Pascanu, R., Lai, M., Jimenez Rezende, D., *et al.*: Interaction networks for learning about objects, relations and physics. In: NeurIPS (2016)
- [25] Marcheggiani, D., Titov, I.: Encoding sentences with graph convolutional networks for semantic role labeling. In: EMNLP (2017)
- [26] Veličković, P., Fedus, W., Hamilton, W.L., Liò, P., Bengio, Y., Hjelm, R.D.: Deep graph infomax. In: ICLR (2018)
- [27] Scarselli, F., Gori, M., Tsoi, A.C., Hagenbuchner, M., Monfardini, G.: The graph neural network model. *IEEE transactions on neural networks* (2008)
- [28] Bruna, J., Zaremba, W., Szlam, A., LeCun, Y.: Spectral networks and deep locally connected networks on graphs. In: ICLR (2014)
- [29] Defferrard, M., Bresson, X., Vandergheynst, P.: Convolutional neural networks on graphs with fast localized spectral filtering. In: NeurIPS (2016)
- [30] Sukhbaatar, S., Fergus, R., *et al.*: Learning multi-agent communication with backpropagation. In: NeurIPS (2016)
- [31] Kipf, T.N., Welling, M.: Semi-supervised classification with graph convolutional networks. In: ICLR (2017)
- [32] Zhang, C., Song, D., Huang, C., Swami, A., Chawla, N.V.: Heterogeneous graph neural network. In: SIGKDD (2019)
- [33] Wang, X., Ji, H., Shi, C., Wang, B., Ye, Y., Cui, P., Yu, P.S.: Heterogeneous graph attention network. In: WWW (2019)
- [34] Gong, L., Cheng, Q.: Exploiting edge features for graph neural networks. In: CVPR (2019)
- [35] Wang, K., Han, C., Long, S., Poon, J.: Megen: Multi-dimensional edge-embedded graph convolutional networks for semi-supervised text classification. In: ICLRW (2022)
- [36] Xiong, C., Li, W., Liu, Y., Wang, M.: Multi-dimensional edge features graph neural network on few-shot image classification. *IEEE Signal Processing Letters* (2021)
- [37] Dwivedi, V.P., Joshi, C.K., Laurent, T., Bengio, Y., Bresson, X.: Benchmarking graph neural networks. arXiv preprint arXiv:2003.00982 (2020)
- [38] Veličković, P., Cucurull, G., Casanova, A., Romero, A., Liò, P., Bengio, Y.: Graph attention networks. In: ICLR (2018)
- [39] Bresson, X., Laurent, T.: Residual Gated Graph ConvNets. arXiv e-prints (2017)
- [40] Luo, C., Song, S., Xie, W., Shen, L., Gunes, H.: Learning multi-dimensional edge feature-based au relation graph for facial action unit recognition. In: IJCAI (2022)
- [41] Shi, L., Zhang, Y., Cheng, J., Lu, H.: Skeleton-based action recognition with directed graph neural networks. In: CVPR (2019)

- [42] Zhong, H., Wu, J., Chen, C., Huang, J., Deng, M., Nie, L., Lin, Z., Hua, X.-S.: Graph contrastive clustering. In: ICCV (2021)
- [43] Pan, E., Kang, Z.: Multi-view contrastive graph clustering. In: NeurIPS (2022)
- [44] Ji, Q., Li, J., Hu, J., Wang, R., Zheng, C., Xu, F.: Rethinking dimensional rationale in graph contrastive learning from causal perspective. arXiv preprint arXiv:2312.10401 (2023)
- [45] Alsentzer, E., Finlayson, S., Li, M., Zitnik, M.: Subgraph neural networks. In: NeurIPS (2020)
- [46] Sun, Q., Li, J., Peng, H., Wu, J., Ning, Y., Yu, P.S., He, L.: Sugar: Subgraph neural network with reinforcement pooling and self-supervised mutual information mechanism. In: WWW (2021)
- [47] Meng, C., Mouli, S.C., Ribeiro, B., Neville, J.: Subgraph pattern neural networks for high-order graph evolution prediction. In: AAAI (2018)
- [48] Zhang, Z., Chen, D., Wang, J., Bai, L., Hancock, E.R.: Quantum-based subgraph convolutional neural networks. PR (2019)
- [49] Wang, X., Zhang, M.: Glass: Gnn with labeling tricks for subgraph representation learning. In: ICLR (2022)
- [50] Chen, D., O’Bray, L., Borgwardt, K.: Structure-aware transformer for graph representation learning. In: ICML (2022)
- [51] Kipf, T.N., Welling, M.: Semi-supervised classification with graph convolutional networks. arXiv preprint arXiv:1609.02907 (2016)
- [52] Hamilton, W., Ying, Z., Leskovec, J.: Inductive representation learning on large graphs. *Advances in neural information processing systems* **30** (2017)
- [53] Veličković, P., Cucurull, G., Casanova, A., Romero, A., Lio, P., Bengio, Y.: Graph attention networks. arXiv preprint arXiv:1710.10903 (2017)
- [54] Wu, F., Souza, A., Zhang, T., Fifty, C., Yu, T., Weinberger, K.: Simplifying graph convolutional networks. In: International Conference on Machine Learning, pp. 6861–6871 (2019). PMLR
- [55] Xu, K., Li, C., Tian, Y., Sonobe, T., Kawarabayashi, K.-i., Jegelka, S.: Representation learning on graphs with jumping knowledge networks. In: International Conference on Machine Learning, pp. 5453–5462 (2018). PMLR
- [56] Xu, K., Hu, W., Leskovec, J., Jegelka, S.: How powerful are graph neural networks? In: International Conference on Learning Representations (2018)
- [57] Morris, C., Ritzert, M., Fey, M., Hamilton, W.L., Lenssen, J.E., Rattan, G., Grohe, M.: Weisfeiler and leman go neural: Higher-order graph neural networks. In: AAAI (2019)
- [58] Wang, Y., Sun, Y., Liu, Z., Sarma, S.E., Bronstein, M.M., Solomon, J.M.: Dynamic graph cnn for learning on point clouds. In: Proceedings of the IEEE/CVF Conference on Computer Vision and Pattern Recognition, pp. 6410–6419 (2019)
- [59] Ma, J., Cui, Q., Kuang, K., Wang, Y., Tang, J.: Path-augmented graph transformer network. In: Proceedings of the Web Conference 2021, pp. 2063–2074 (2021)
- [60] Li, Y., Ouyang, W., Zhou, B., Wang, K., Wang, X.: Scene graph generation from objects, phrases and region captions. In: Proceedings of the IEEE International Conference on Computer Vision, pp. 1261–1270 (2017)
- [61] Han, K., Wang, Y., Guo, J., Tang, Y., Wu, E.: Vision gnn: An image is worth graph of nodes. *Advances in neural information processing systems* **35**, 8291–8303 (2022)
- [62] Wang, X., Gupta, A.: Videos as space-time region graphs. In: Proceedings of the European Conference on Computer Vision (ECCV) (2018)
- [63] Chen, Y., Zhang, Z., Yuan, C., Li, B., Deng, Y., Hu, W.: Channel-wise topology refinement graph convolution for skeleton-based action recognition. In: ICCV (2021)
- [64] Purwins, H., Li, B., Virtanen, T., Schlüter, J., Chang, S.-Y., Sainath, T.: Deep learning for audio signal processing. *IEEE Journal of Selected Topics in Signal Processing* **13**(2), 206–219 (2019) <https://doi.org/10.1109/JSTSP.2019.2908700>
- [65] Shirian, A., Somandepalli, K., Guha, T.: Self-supervised graphs for audio representation learning with limited labeled data. *IEEE Journal of Selected Topics in Signal Processing*

16(6), 1391–1401 (2022)

- [66] Zhang, S., Qin, Y., Sun, K., Lin, Y.: Few-shot audio classification with attentional graph neural networks. In: *Interspeech*, pp. 3649–3653 (2019)
- [67] Singh, S., Steinmetz, C.J., Benetos, E., Phan, H., Stowell, D.: Atggnn: Audio tagging graph neural network. *IEEE Signal Processing Letters* (2024)
- [68] Abbas, S., Ojo, S., Al Hejaili, A., Sampetro, G.A., Almadhor, A., Zaidi, M.M., Kryvinska, N.: Artificial intelligence framework for heart disease classification from audio signals. *Scientific Reports* **14**(1), 3123 (2024)
- [69] Kürzinger, L., Lindae, N., Klewitz, P., Rigoll, G.: Lightweight end-to-end speech recognition from raw audio data using sinc-convolutions. *arXiv preprint arXiv:2010.07597* (2020)
- [70] Huang, J., Wu, W., Li, J., Wang, S.: Text summarization method based on gated attention graph neural network. *Sensors* **23**(3), 1654 (2023)
- [71] Wimalawarne, K., Suzuki, T.: Layer-wise adaptive graph convolution networks using generalized pagerank. In: *Asian Conference on Machine Learning*, pp. 1117–1132 (2023). PMLR
- [72] Brody, S., Alon, U., Yahav, E.: How attentive are graph attention networks? In: *International Conference on Learning Representations* (2021)
- [73] Simonovsky, M., Komodakis, N.: Dynamic edge-conditioned filters in convolutional neural networks on graphs. In: *Proceedings of the IEEE Conference on Computer Vision and Pattern Recognition*, pp. 3693–3702 (2017)
- [74] Cui, S., Yu, B., Liu, T., Zhang, Z., Wang, X., Shi, J.: Edge-enhanced graph convolution networks for event detection with syntactic relation. *arXiv preprint arXiv:2002.10757* (2020)
- [75] Shang, C., Liu, Q., Chen, K.-S., Sun, J., Lu, J., Yi, J., Bi, J.: Edge attention-based multi-relational graph convolutional networks. *arXiv preprint arXiv: 1802.04944* (2018)
- [76] Schlichtkrull, M., Kipf, T.N., Bloem, P., Van Den Berg, R., Titov, I., Welling, M.: Modeling relational data with graph convolutional networks. In: *The Semantic Web: 15th International Conference, ESWC 2018, Heraklion, Crete, Greece, June 3–7, 2018, Proceedings 15*, pp. 593–607 (2018). Springer
- [77] LeCun, Y., Bottou, L., Bengio, Y., Haffner, P.: Gradient-based learning applied to document recognition. *Proceedings of the IEEE* (1998)
- [78] Krizhevsky, A., Hinton, G., et al.: Learning multiple layers of features from tiny images (2009)
- [79] Zhao, W., Xu, C., Cui, Z., Zhang, T., Jiang, J., Zhang, Z., Yang, J.: When work matters: Transforming classical network structures to graph cnn. *arXiv preprint arXiv:1807.02653* (2018)
- [80] Dobson, P.D., Doig, A.J.: Distinguishing enzyme structures from non-enzymes without alignments. *Journal of molecular biology* **330**(4), 771–783 (2003)
- [81] Gallicchio, C., Micheli, A.: Fast and deep graph neural networks. In: *Proceedings of the AAAI Conference on Artificial Intelligence*, vol. 34, pp. 3898–3905 (2020)
- [82] Irwin, J.J., Sterling, T., Mysinger, M.M., Bolstad, E.S., Coleman, R.G.: Zinc: a free tool to discover chemistry for biology. *Journal of chemical information and modeling* (2012)
- [83] Sorkun, M.C., Khetan, A., Er, S.: Aqsolddb, a curated reference set of aqueous solubility and 2d descriptors for a diverse set of compounds. *Scientific data* (2019)
- [84] Joshi, C.K., Cappart, Q., Rousseau, L.-M., Laurent, T.: Learning the travelling salesperson problem requires rethinking generalization. *Constraints* (2022)
- [85] Li, G., Xiong, C., Thabet, A., Ghanem, B.: Deepergcn: All you need to train deeper gcn. *arXiv preprint arXiv:2006.07739* (2020)
- [86] Hu, W., Fey, M., Zitnik, M., Dong, Y., Ren, H., Liu, B., Catasta, M., Leskovec, J.: Open graph benchmark: Datasets for machine learning on graphs. In: *NeurIPS* (2020)
- [87] Xu, K., Hu, W., Leskovec, J., Jegelka, S.: How powerful are graph neural networks? In: *ICLR* (2018)
- [88] Morris, C., Rattan, G., Mutzel, P.: Weisfeiler and leman go sparse: Towards scalable higher-order graph embeddings. *Advances in Neural Information Processing Systems* **33**, 21824–21840 (2020)

- [89] Corso, G., Cavalleri, L., Beaini, D., Liò, P., Veličković, P.: Principal neighbourhood aggregation for graph nets. In: *NeurIPS* (2020)
- [90] Beaini, D., Passaro, S., Létourneau, V., Hamilton, W., Corso, G., Liò, P.: Directional graph networks. In: *ICML* (2021)
- [91] Hussain, M.S., Zaki, M.J., Subramanian, D.: Global self-attention as a replacement for graph convolution. In: *KDD* (2022)
- [92] Cai, S., Li, L., Han, X., Luo, J., Zha, Z.-J., Huang, Q.: Automatic relation-aware graph network proliferation. In: *CVPR* (2022)
- [93] Shirzad, H., Velingker, A., Venkatachalam, B., Sutherland, D.J., Sinop, A.K.: Expformer: Sparse transformers for graphs. *arXiv preprint arXiv:2303.06147* (2023)
- [94] Cai, S., Li, L., Deng, J., Zhang, B., Zha, Z.-J., Su, L., Huang, Q.: Rethinking graph neural architecture search from message-passing. In: *CVPR* (2021)
- [95] Li, M., Chen, S., Chen, X., Zhang, Y., Wang, Y., Tian, Q.: Actional-structural graph convolutional networks for skeleton-based action recognition. In: *CVPR* (2019)
- [96] Zhang, P., Lan, C., Zeng, W., Xing, J., Xue, J., Zheng, N.: Semantics-guided neural networks for efficient skeleton-based human action recognition. In: *CVPR* (2020)
- [97] Plizzari, C., Cannici, M., Matteucci, M.: Skeleton-based action recognition via spatial and temporal transformer networks. *CVIU* (2021)
- [98] Cheng, K., Zhang, Y., He, X., Chen, W., Cheng, J., Lu, H.: Skeleton-based action recognition with shift graph convolutional network. In: *CVPR* (2020)
- [99] Cheng, K., Zhang, Y., Cao, C., Shi, L., Cheng, J., Lu, H.: Decoupling gcn with dropgraph module for skeleton-based action recognition. In: *ECCV* (2020)
- [100] Ye, F., Pu, S., Zhong, Q., Li, C., Xie, D., Tang, H.: Dynamic gcn: Context-enriched topology learning for skeleton-based action recognition. In: *ACM MM* (2020)
- [101] Liu, Z., Zhang, H., Chen, Z., Wang, Z., Ouyang, W.: Disentangling and unifying graph convolutions for skeleton-based action recognition. In: *CVPR* (2020)
- [102] Chen, Z., Li, S., Yang, B., Li, Q., Liu, H.: Multi-scale spatial temporal graph convolutional network for skeleton-based action recognition. In: *AAAI* (2021)
- [103] Chi, H.-g., Ha, M.H., Chi, S., Lee, S.W., Huang, Q., Ramani, K.: Infogcn: Representation learning for human skeleton-based action recognition. In: *CVPR* (2022)
- [104] Lee, J., Lee, M., Lee, D., Lee, S.: Hierarchically decomposed graph convolutional networks for skeleton-based action recognition. In: *Proceedings of the IEEE/CVF International Conference on Computer Vision*, pp. 10444–10453 (2023)
- [105] Rampásek, L., Galkin, M., Dwivedi, V.P., Luu, A.T., Wolf, G., Beaini, D.: Recipe for a general, powerful, scalable graph transformer. *Advances in Neural Information Processing Systems* **35**, 14501–14515 (2022)
- [106] Yang, M., Shen, Y., Qi, H., Yin, B.: Breaking the Expressive Bottlenecks of Graph Neural Networks (2020)
- [107] Kong, K., Li, G., Ding, M., Wu, Z., Zhu, C., Ghanem, B., Taylor, G., Goldstein, T.: Robust optimization as data augmentation for large-scale graphs. In: *Proceedings of the IEEE/CVF Conference on Computer Vision and Pattern Recognition*, pp. 60–69 (2022)